

Deep Learning-Based Synchronization for Uplink NB-IoT

Fayçal Aït Aoudia, Jakob Hoydis, Sebastian Cammerer,
Matthijs Van Keirsbilck, and Alexander Keller
NVIDIA
Contact: faitaoudia@nvidia.com

Abstract—We propose a neural network (NN)-based algorithm for device detection and time of arrival (ToA) and carrier frequency offset (CFO) estimation for the narrowband physical random-access channel (NPRACH) of narrowband internet of things (NB-IoT). The introduced NN architecture leverages residual convolutional networks as well as knowledge of the preamble structure of the 5G New Radio (5G NR) specifications. Benchmarking on a 3rd Generation Partnership Project (3GPP) urban microcell (UMi) channel model with random drops of users against a state-of-the-art baseline shows that the proposed method enables up to 8 dB gains in false negative rate (FNR) as well as significant gains in false positive rate (FPR) and ToA and CFO estimation accuracy. Moreover, our simulations indicate that the proposed algorithm enables gains over a wide range of channel conditions, CFOs, and transmission probabilities. The introduced synchronization method operates at the base station (BS) and, therefore, introduces no additional complexity on the user devices. It could lead to an extension of battery lifetime by reducing the preamble length or the transmit power. Our code is available at: https://github.com/NVlabs/nprach_synch/.

I. INTRODUCTION

Narrowband internet of things (NB-IoT) is a radio technology standard developed by the 3rd Generation Partnership Project (3GPP) to enable a wide range of IoT services and user equipments (UEs) [1]. It mostly reuses 5G New Radio (5G NR) specifications, and aims to support massive numbers of connected UEs and to provide very good outdoor-to-indoor coverage, very low power consumption to enable long battery lifetime, and low cost connectivity. In the uplink, many UEs can simultaneously contend to access the channel in a random access manner. The narrowband physical random-access channel (NPRACH) relates to the first message sent by a UE to a base station (BS) to request access to the channel, and is used by the BS to identify the UE and estimate its time of arrival (ToA) and carrier frequency offset (CFO).

The NPRACH waveform [2] is specified as a single-tone frequency hopping preamble, and different con-

figurations are available to adapt to various channel conditions and cell sizes. Frequency hopping is performed according to a pseudo-random pattern to mitigate inter-cell interference as neighboring cells use different hopping patterns. Within a cell, up to 48 orthogonal hopping patterns are available for the UEs to choose from, and the UEs that simultaneously request access to the channel must use different patterns to avoid collisions. The problem of NPRACH detection consists in jointly detecting the UEs that simultaneously attempt to access the channel and estimating their respective ToAs and CFOs.

To make the problem tractable, many existing algorithms [3]–[5] assume that (i) the channel frequency response is flat, which is reasonable considering the narrow bandwidth of NB-IoT (180 kHz), (ii) interference between UEs can be neglected, which only holds true assuming low CFO and low mobility, and (iii) the channel is time-invariant over the duration of the preamble, which is only valid under low mobility. Moreover, most algorithms require the configuration of a detection power threshold that depends on the noise-plus-interference level, and which controls the trade-off between the occurrence of false positives and false negatives.

We propose a deep learning-based synchronization algorithm that requires none of these assumptions to hold, as well as no configuration of a detection threshold. The proposed algorithm is standard-compliant and operates at the BS, leading to no additional complexity for the UEs. To the best of our knowledge, the only related work is [6], which uses a convolutional neural network to predict the active UEs and corresponding ToAs and CFOs. In comparison, the method we propose uses a different neural network (NN) architecture which exploits knowledge of the preamble structure to achieve increased performance. Moreover, it uses a different loss function for training which is key to enable accurate ToA and CFO estimates.

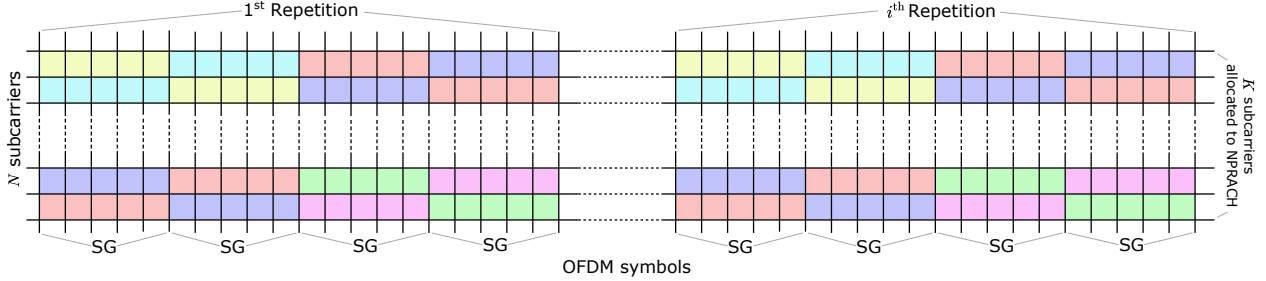


Fig. 1: NPRACH structure. Each color correspond to a preamble transmitted by a user.

Benchmarking using the Sionna link-level simulator [7] on a realistic 3GPP urban microcell (UMi) channel model [8] and against a state-of-the-art baseline [5] shows that the proposed algorithm enables gains of up to 8 dB in false negative rate (FNR), significant reduction in false positive rate (FPR), and more accurate ToA and CFO estimation. Moreover, these results hold over a wide range of CFOs and transmission probabilities. As these gains were obtained for a short preamble length, such an algorithm may remove the need for longer preambles under many channel conditions or reduce the required transmit power, leading to battery lifetime extension which is critical for NB-IoT applications.

II. SYSTEM MODEL

The NPRACH waveform [2] consists of a sequence of symbol groups (SGs), as shown in Fig. 1. Each SG is made of five identical single-tone orthogonal frequency division multiplexing (OFDM) symbols that share a single cyclic prefix (CP) to reduce overhead, and occupies one tone of 3.75 kHz bandwidth. Frequency hopping is performed between the SGs, and four consecutive SGs are treated as the basic unit of the preamble, referred to as a *repetition*. A preamble can consist of up to 128 repetitions for coverage extension.

Let us denote by K the maximum number of devices that can simultaneously access the channel. It is assumed that UEs that simultaneously request access do not collide, i.e., that they use different hopping patterns. Some methods in the literature address the detection of colliding UEs, e.g., [9]. However, there is currently no procedure to acknowledge access requests from colliding UEs. Under this assumption, the highest value allowed for K is 48, as this is the highest number of hopping patterns available [2]. The samples transmitted by the k^{th} user for the i^{th} symbol of the m^{th} SG is

$$s_{k,m,i}[n] = \beta_k e^{j2\pi\phi_k[m]\frac{n}{N}} \quad (1)$$

where β_k is the transmission power used by the k^{th} user, N is the number of subcarriers, and $\phi_k[m]$ is the subcarrier index used by the k^{th} user for the m^{th} SG and is determined by the hopping pattern. Note that N is typically greater than K as the NPRACH is only part of the radio spectrum processed by the BS.

We consider a multi-user time-invariant multipath channel, where the channel response of the k^{th} user is

$$h_k(\tau) = \sum_{p=0}^{P_k-1} a_{k,p} \delta(\tau - \tau_{k,p}) \quad (2)$$

where P_k is the number of paths for the k^{th} user, and $a_{k,p}$ and $\tau_{k,p}$ are the baseband coefficient and delay of the p^{th} path of the k^{th} user, respectively. The ToA of the k^{th} user is defined as

$$D_k := \min_p \tau_{k,p}. \quad (3)$$

The received signal at the BS is

$$y_{m,i}[n] = \sum_{k=0}^{K-1} \sum_{\ell=-\infty}^{\infty} A_k h_{k,\ell} s_{k,m,i}[n-\ell] e^{j2\pi f_{\text{off},k}(n-\ell)} + w_{m,i}[n] \quad (4)$$

where A_k indicates if user k is active, i.e., it equals 1 if the user is transmitting and 0 otherwise, $h_{k,\ell}$ is the channel coefficient of the ℓ^{th} tap and of the k^{th} user, $f_{\text{off},k}$ is the CFO of the k^{th} user normalized by the sampling frequency, and $w_{m,i}[n]$ is the additive white Gaussian noise (AWGN) with variance σ^2 . To simulate the channel, summation over taps is performed for a finite number of time-lags $L_{\min} \leq \ell \leq L_{\max}$. Assuming sinc pulse shaping on the transmitter side and matched filtering on the receiver side, the channel taps are

$$h_{k,\ell} = \sum_{p=0}^{P_k-1} a_{k,p} \text{sinc}(\ell - W\tau_{k,p}) \quad (5)$$

$$= \mathcal{F}^{-1} \{ \text{rect}(f) H_k(f) \} (\ell) \quad (6)$$

where $W = N\Delta_f$ is the bandwidth, $\mathcal{F}^{-1}\{X(f)\}(t)$ the inverse Fourier transform of $X(f)$ evaluated at t , and

$$H_k(f) = \sum_{p=0}^{P_k-1} a_{k,p} e^{-j2\pi\tau_{k,p}Wf} \quad (7)$$

the frequency response of the channel.

On the receiver side, the CP of each SG is removed and discrete Fourier transform (DFT) is performed. This leads to a resource grid (RG) \mathbf{Y} of size $N \times 5S$ where S is the number of SGs forming the preamble. Considering the k^{th} user, the received signal for the i^{th} symbol of the m^{th} SG is

$$\begin{aligned} Y[\phi_k[m], 5m+i] &= A_k H_k \left(\frac{\phi_k[m]}{N} \right) \beta_k \cdot \\ \frac{1}{N} \sum_{n=N_{m,i}}^{N_{m,i}+N-1} e^{j2\pi f_{\text{off},k}n} &+ \sum_{k' \neq k} \left\{ A_{k'} H_{k'} \left(\frac{\phi_k[m]}{N} \right) \beta_{k'} \cdot \right. \\ \frac{1}{N} \sum_{n=N_{m,i}}^{N_{m,i}+N-1} e^{j2\pi \left(\frac{\phi_{k'}[m] - \phi_k[m]}{N} + f_{\text{off},k'} \right) n} &\left. \right\} \\ &+ W_{k,m,i}[\phi_k[m], 5m+i] \quad (8) \end{aligned}$$

where $W[\phi_k[m], 5m+i]$ is AWGN with variance σ^2 , and $N_{m,i} := mN_{\text{SG}} + iN$ where N_{SG} is the number of samples forming an SG. The hopping patterns are orthogonal in time and frequency, i.e., $\phi_k[m] \neq \phi_{k'}[m]$ when $k \neq k'$. The first term on the right-hand side of (8) is the signal received from the k^{th} user, and the second term corresponds to inter-carrier interference (ICI) from the other users due to CFO. NPRACH synchronization consists in jointly detecting the active users and estimating their ToA and CFO from the received signal \mathbf{Y} (8). The next section introduces a NN-based detector that aims to achieve this goal by exploiting the NPRACH preamble structure.

III. DEEP LEARNING-BASED SYNCHRONIZATION

Fig. 2 shows the algorithm that we propose for NPRACH synchronization. It takes as input the received RG $\mathbf{Y} \in \mathbb{C}^{N \times 5S}$, which is first preprocessed into a real-valued tensor $\bar{\mathbf{Y}} \in \mathbb{R}^{K \times S \times 3}$. $\bar{\mathbf{Y}}$ then serves as input to two NNs, one to compute transmission probabilities, denoted by $\widehat{\text{Pr}}(A_k | \bar{\mathbf{Y}})$, and the other to compute ToA and CFO estimates, denoted by \widehat{D}_k and $\widehat{f}_{\text{off},k}$, respectively. The rest of this section details the preprocessing, the NN architectures, and the loss function used for training.

A. Preprocessing

Preprocessing consists of first averaging the five resource elements (REs) forming each SG. This is done

separately for each subcarrier. This preprocessing step reduces by a factor of five the input size, resulting in a matrix $\tilde{\mathbf{Y}} \in \mathbb{C}^{N \times S}$.

The second preprocessing step consists of separately normalizing the sequences of SGs corresponding to the K possible hopping patterns. This is key to enable accurate detection despite the users having signal-to-noise ratios (SNRs) that differ by orders of magnitude due to path loss. This is achieved by gathering the K sequences corresponding to every hopping pattern $\tilde{\mathbf{y}}_k \in \mathbb{C}^S$, $0 \leq k \leq K-1$, according to the 3GPP specifications [2], and normalizing each sequence individually. The resulting normalized sequences are then converted from complex-valued tensors to real-valued ones by stacking the real and imaginary components along an additional dimension, resulting in a tensor of shape $S \times 2$. As normalization erases the information about the received power, the average received power of each sequence is computed prior to normalization in log-scale and concatenated to the normalized sequence along the inner dimension. The received power takes values over a range of several orders of magnitude due to path loss. Finally, the K resulting tensors are scattered according to the hopping patterns, reverting the previous gathering operation, to form a normalized tensor $\bar{\mathbf{Y}} \in \mathbb{R}^{K \times S \times 3}$. This allows the NNs to operate over the time-frequency RG and hence to better mitigate the ICI due to CFO, as opposed to conventional approaches which typically ignore ICI for tractability.

B. Neural Network Architecture

The tensor $\bar{\mathbf{Y}}$ serves as input to two NNs that share a similar architecture. For each user, the first NN computes a probability of the user to request channel access, and the second NN computes estimates of the ToA and the CFO of the user. The first stage of both NNs is motivated by the ICI caused by the CFO, and consists of one-dimensional (1D) depth-wise separable convolutional layers [10] with 128 kernels of size 3 and that operate along the frequency dimension. Depth-wise separable convolutional layers are used as they significantly decrease computational complexity compared to conventional convolutional layers without reducing accuracy. Skip connections are used to avoid gradient vanishing, and zero-padding ensures that the output has the same length as the input. The resulting tensors are denoted by $\mathbf{Z}^{(1)}$ and $\mathbf{Z}^{(2)}$ for the first and second NN, respectively, and have shape $K \times S \times 128$, where the last dimension corresponds to the ‘‘channels’’ of the convolution. Intuitively, the convolutional NNs compute for each subcarrier and for each SG a vector of features.

Next, the sequences of SGs corresponding to the hopping patterns are gathered, leading to K tensors denoted by $\mathbf{Z}_k^{(1)} \in \mathbb{R}^{S \times 128}$ and $\mathbf{Z}_k^{(2)} \in \mathbb{R}^{S \times 128}$, $0 \leq k \leq K-1$, for the first and second NN, respectively. This operation is similar to the one performed for normalizing the received NN at preprocessing. The first NN computes for every user k a probability that the user is requesting channel access, denoted by $\widehat{\Pr}(A_k|\bar{\mathbf{Y}})$, by processing $\mathbf{Z}_k^{(1)}$ with a multilayer perceptron (MLP). Similarly, the second NN computes for every user k estimates of the ToA and CFO, denoted by \widehat{D}_k and $\widehat{f}_{\text{off},k}$, from $\mathbf{Z}_k^{(2)} \in \mathbb{R}^{S \times 128}$ using two separate MLPs. For both NNs, weights sharing is performed across the K hopping patterns for the MLPs.

The use of MLPs is made possible as short preambles are assumed, leading to small values of S . For example, one preamble repetition corresponds to $S = 4$. Long preambles could prohibit the use of MLPs due to scalability and require a different architecture. However, as we will see in the next section, the proposed algorithm enables significant gains that could remove the need for longer preambles in many environments.

C. Loss Function

Training of the NN that detects the transmitting users is done on the binary cross-entropy

$$\mathcal{L}_1 := - \sum_{k=0}^{K-1} \mathbb{E} \left[\ln \left(\widehat{\Pr}(A_k|\bar{\mathbf{Y}}) \right) \right] \quad (9)$$

which is estimated through Monte Carlo sampling by

$$\begin{aligned} \mathcal{L}_1 \approx & -\frac{1}{B} \sum_{b=1}^{B-1} \sum_{k=0}^{K-1} \left[A_k^{[b]} \ln \left(\widehat{\Pr}(A_k^{[b]}|\bar{\mathbf{Y}}^{[b]}) \right) \right. \\ & \left. + \left(1 - A_k^{[b]} \right) \ln \left(1 - \widehat{\Pr}(A_k^{[b]}|\bar{\mathbf{Y}}^{[b]}) \right) \right] \end{aligned} \quad (10)$$

where B is the batch size and the superscript $[b]$ refers to the b^{th} batch example.

Training of the NN that estimates ToA and CFO is done on the weighted mean squared error

$$\begin{aligned} \mathcal{L}_2 := & \sum_{k=0}^{K-1} \mathbb{E} \left[A_k \text{SNR}_k \left(D_k - \widehat{D}_k \right)^2 \right] \\ & + \sum_{k=0}^{K-1} \mathbb{E} \left[A_k \text{SNR}_k \left(f_{\text{off},k} - \widehat{f}_{\text{off},k} \right)^2 \right] \end{aligned} \quad (11)$$

where

$$\text{SNR}_k := \frac{\beta_k}{\sigma^2} \frac{1}{S} \sum_{m=0}^{S-1} \left| H_k \left(\frac{\phi_k[m]}{N} \right) \right|^2 \quad (12)$$

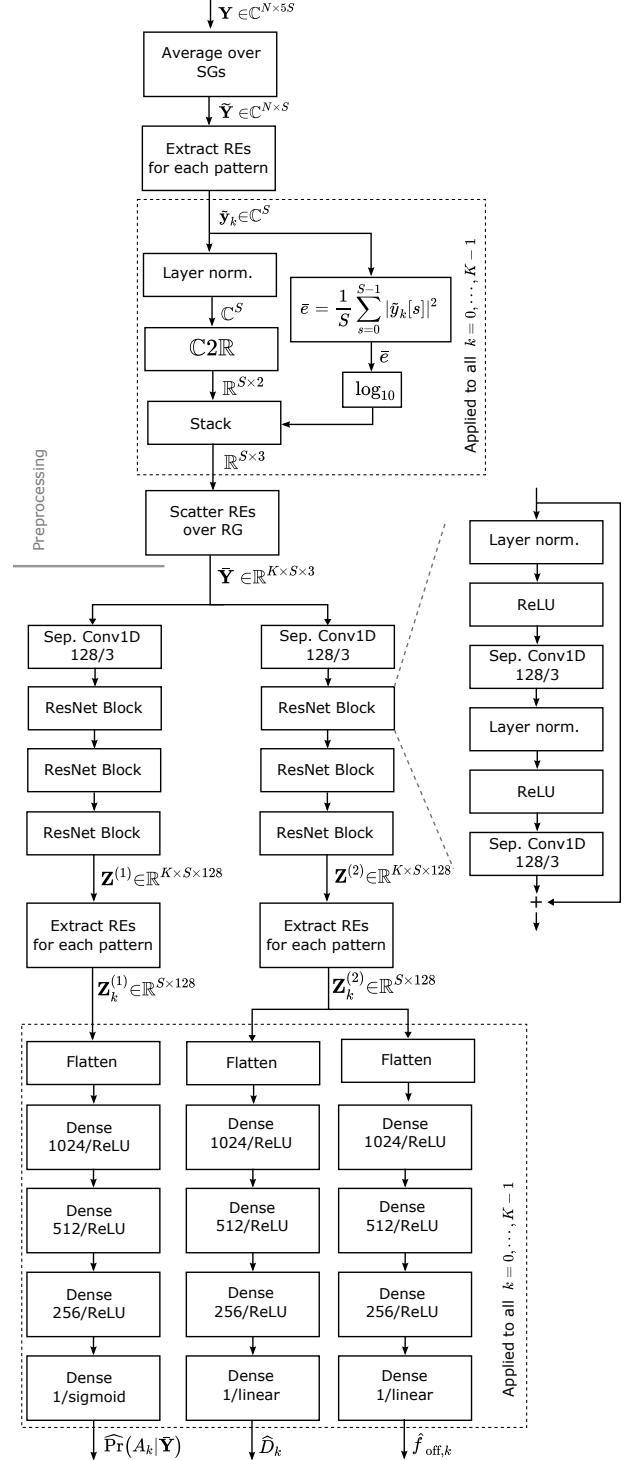


Fig. 2: NN-based synchronization algorithm. When labeling the output of a layer is not required, only the shape is indicated. For dense layers, the number of units/activation function is indicated. For separable convolution layers, the number of kernels/kernel size is indicated.

is the average SNR of user k . Weighting by A_k ensures that only the active users are considered. Weighting by the SNR is motivated by the observation that the errors measured for high SNRs are negligible compared to the ones measured for low SNRs. Training on the unweighted MSE therefore results in poor accuracy for high SNR. The loss \mathcal{L}_2 is estimated by

$$\mathcal{L}_2 \approx \frac{1}{B} \sum_{k=0}^{K-1} \sum_{b=0}^{B-1} A_k^{[b]} \text{SNR}_k^{[b]} \left(D_k^{[b]} - \widehat{D}_k^{[b]} \right)^2 + \frac{1}{B} \sum_{k=0}^{K-1} \sum_{b=0}^{B-1} A_k^{[b]} \text{SNR}_k^{[b]} \left(f_{\text{off},k}^{[b]} - \widehat{f}_{\text{off},k}^{[b]} \right)^2. \quad (13)$$

Training of the two NNs is jointly performed on the total loss

$$\mathcal{L} := \mathcal{L}_1 + \mathcal{L}_2 \quad (14)$$

where no weighting is required as \mathcal{L}_1 and \mathcal{L}_2 act on different NNs.

IV. SIMULATIONS RESULTS

We have benchmarked the previously described algorithm against a state-of-the-art baseline using the Sionna link-level simulator [7]. The 3GPP UMi channel model [8] was used, with the carrier frequency set to 3.4 GHz and the sampling frequency set to 50 MHz. The NPRACH preamble format 0 was implemented, and the number of repetitions was set to 1, leading to $S = 4$ SGs. Following the NB-IoT specifications [2], the subcarrier spacing Δ_f was set to 3.75 kHz and the number of subcarriers allocated to the NPRACH to 48. The maximum number of users that can simultaneously request channel access was set to $K = 48$ with collisionless access. Note that the proposed method could be trained to detect and resolve collisions. However, as there is no procedure for handling collisions, such a solution could not be exploited.

Training of the NNs was done using the Adam optimizer [11], with the batch size set to 64 and the learning rate set to 10^{-3} . At training, the probability for a user to request access $P(A_k)$ was independently and uniformly sampled from the range $(0, 1)$ for each batch example. The CFO, in parts-per-million (ppm), of each user and for each batch example was independently and uniformly sampled from the range $(-25, 25)$. Similarly, the ToA of each user and for each batch example was independently and uniformly sampled from the range $(0, 66.7 \mu\text{s})$, where $66.7 \mu\text{s}$ corresponds to the CP length [2]. The ToAs were added to the path delays generated by the 3GPP UMi channel model. At both evaluation and training, each batch example consisted

of a random drop of K users with randomly chosen large scale parameters to avoid over-fitting to specific channel conditions. Note that a *single* NN was trained over a wide range of transmission probabilities, CFOs, and channel conditions, and then evaluated under specific conditions.

To benchmark the proposed method, the synchronization algorithm from [5] was implemented, which builds on previous work [3], [4]. This algorithm relies on the configuration of a detection power threshold denoted by γ , that controls a trade-off between the FNR and the FPR. As in [5], the size of the fast Fourier transform (FFT) performed by the baseline was set to 256. Moreover, two values for the detection threshold were used, corresponding to false alarm probabilities of 99.9% (as in [5]) and 99%.

Fig. 3a shows FNR versus SNR (12). In all figures, the baseline and our approach are referred to as ‘‘BL’’ and ‘‘NN’’, respectively. The CFO was randomly and uniformly sampled for each user, and the maximum CFO value in ppm is indicated in the legend. The probability for a user to transmit was set to 0.5 for Figures 3a to 3c. One can see that the NN-based method enables gains of up to 8 dB at an FNR of 10^{-3} under no CFO. The gains decrease as the CFO increases, but remain significant even under high CFOs of up to 20 ppm. As expected, the FNRs achieved by the baseline are slightly better for the low power detection threshold γ . However, this is at the cost of higher FPRs, as shown in Fig. 3e. Note that Fig. 3e shows results averaged over all channel realizations, and therefore over all SNRs. The FPR is significantly higher with the baseline than with the NN approach, except for the lowest CFOs. The steep FPR increase observed for the baseline can be explained by the ICI caused by the CFO (8), as the energy leaked in adjacent subcarriers erroneously triggers the detection threshold. The more advanced processing performed by the NN-based partially prevents from false detection.

In addition to better detection performance, the NN-based algorithm also enables more accurate ToA and CFO estimation, as shown in Fig. 3b and Fig. 3c. For the baseline, the detection threshold γ does not impact the ToA and CFO estimation accuracy. Both the baseline and the NN-based approach are negatively impacted by increasing CFOs, however, the NN-based algorithm outperforms the baseline for all CFO values. Moreover, as shown in Fig 3d, the NN-based algorithm outperforms the baseline in ToA estimation for all transmission probabilities. Similar results were obtained for CFO estimation, but are not shown due to space limitation.

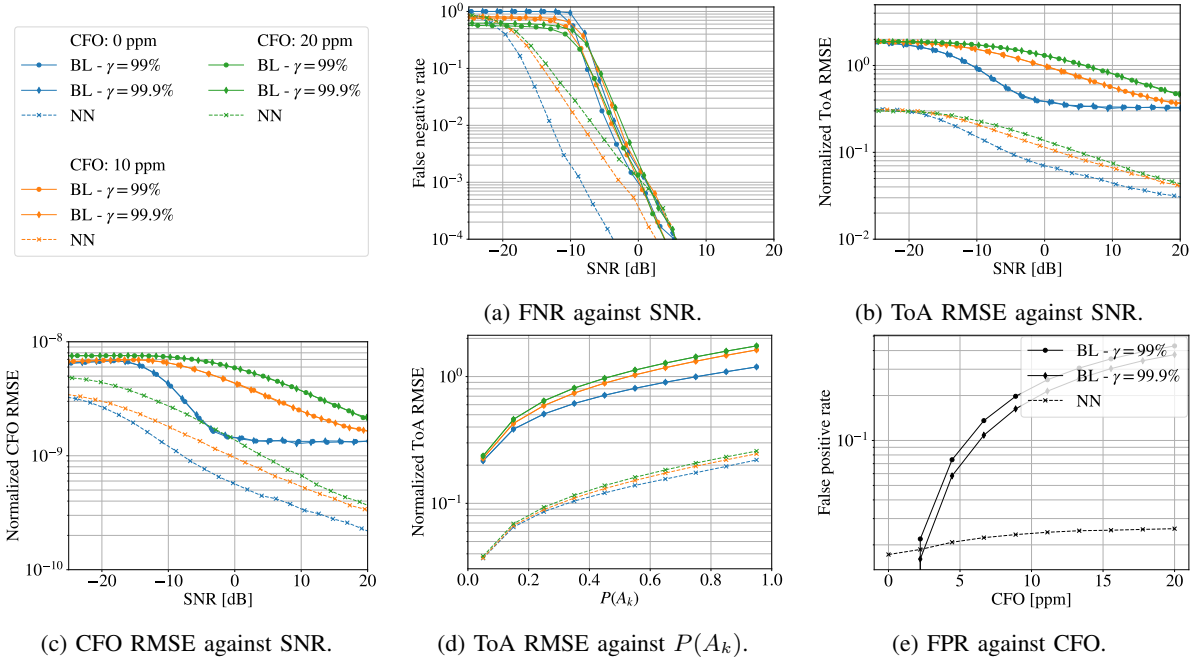


Fig. 3: Simulation results. γ is the baseline detection threshold. $P(A_k)$ is the probability for a user to transmit.

V. CONCLUSION

We have developed a NN based solution for NPRACH synchronization in NB-IoT. We have shown that it enables significant gains in FNR, FPR, as well as ToA and CFO estimation accuracy. These gains are observed for a wide range of CFOs and transmission probabilities, showing the robustness of the such an approach. Our solution is standard-compliant and incurs no additional complexity at the user devices. It could hence increase battery lifetime by enabling shorter preambles or lower transmit power, which is critical for NB-IoT applications.

REFERENCES

- [1] M. Kanj, V. Savaux, and M. Le Guen, "A Tutorial on NB-IoT Physical Layer Design," *IEEE Commun. Surveys Tuts.*, vol. 22, no. 4, pp. 2408–2446, 2020.
- [2] 3rd Generation Partnership Project (3GPP), "Evolved Universal Terrestrial Radio Access (E-UTRA); Physical channels and modulation," *TS 36.211, V17.0.0*, 2022.
- [3] H. Chougrani, S. Kisseleff, and S. Chatzinotas, "Efficient Preamble Detection and Time-of-Arrival Estimation for Single-Tone Frequency Hopping Random Access in NB-IoT," *IEEE Internet Things J.*, vol. 8, no. 9, pp. 7437–7449, 2021.
- [4] X. Lin, A. Adhikary, and Y.-P. Eric Wang, "Random Access Preamble Design and Detection for 3GPP Narrowband IoT Systems," *IEEE Wireless Commun. Lett.*, vol. 5, no. 6, pp. 640–643, 2016.
- [5] A. Chakrapani, "NB-IoT Uplink Receiver Design and Performance Study," *IEEE Internet Things J.*, vol. 7, no. 3, pp. 2469–2482, 2020.
- [6] M. H. Jespersen, M. Pajovic, T. Koike-Akino, Y. Wang, P. Popovski, and P. V. Orlik, "Deep Learning for Synchronization and Channel Estimation in NB-IoT Random Access Channel," in *IEEE Global Telecommun. Conf. (GLOBECOM)*, 2019, pp. 1–7.
- [7] J. Hoydis, S. Cammerer, F. Ait Aoudia, A. Vem, N. Binder, G. Marcus, and A. Keller, "Sionna: An Open-Source Library for Next-Generation Physical Layer Research," *preprint arXiv:2203.11854*, 2022.
- [8] 3rd Generation Partnership Project (3GPP), "Study on channel model for frequencies from 0.5 to 100 GHz," *TS 38.901, V17.0.0*, 2022.
- [9] H. S. Jang, H. Lee, T. Q. S. Quek, and H. Shin, "Deep Learning-Based Cellular Random Access Framework," *IEEE Trans. Wireless Commun.*, vol. 20, no. 11, pp. 7503–7518, 2021.
- [10] F. Chollet, "Xception: Deep Learning With Depthwise Separable Convolutions," in *IEEE Conf. Comput. Vis. Pattern Recog. (CVPR)*, July 2017.
- [11] D. P. Kingma and J. Ba, "Adam: A Method for Stochastic Optimization," *preprint arXiv:1412.6980*, 2014.